



# Electronic helix theory-guided rational design of kinetic resolutions by means of the Sharpless asymmetric dihydroxylation reactions

Xiangyou Xing, Yaohong Zhao, Chen Xu, Xinyang Zhao, David Zhigang Wang\*

Key Laboratory of Chemical Genomics, School of Chemical Biology and Biotechnology, Shenzhen Graduate School of Peking University, Shenzhen University Town, Shenzhen 518055, China

## ARTICLE INFO

### Article history:

Received 18 April 2012  
Received in revised form 7 June 2012  
Accepted 26 June 2012  
Available online 4 July 2012

### Keywords:

Polarizability  
Sharpless asymmetric dihydroxylation  
Electronic helix theory  
Stereochemistry  
Kinetic resolution

## ABSTRACT

Kinetic resolution represents a key chemical reaction strategy for asymmetric synthesis of optically enriched compounds, and it originates from a simple phenomenon that a pair of mirror images (enantiomers) of a racemate can react with different rates under a chiral environment. While highly efficient catalytic kinetic resolutions by means of the classical Sharpless asymmetric epoxidation (AE) reactions are well established in modern organic synthesis, such systems based on the arguably more versatile Sharpless asymmetric dihydroxylation (AD) processes, although long pursued and widely attempted, remain largely underexplored. With insights gained from a new electronic helix theory we recently developed for molecular chirality and chiral interactions, we were able to advance a proposal suggesting why this problem is challenging and how it might be solved. Guided by a new design concept aimed at identifying complimentary catalyst–substrate electronic interactions, we reported herein that not only can such elusive systems be generally feasible, but efficiencies well reach the highest levels known to date with chemical or enzymatic kinetic resolutions of any type.

© 2012 Elsevier Ltd. All rights reserved.

## 1. Introduction

The Sharpless asymmetric dihydroxylation (AD) and Sharpless asymmetric epoxidation (AE) reactions are two fundamentally important chemical transformations<sup>1</sup> that stereoselectively oxidize alkenes into optically enriched products of useful enantiomeric excesses (ees). The enantioselections in these processes can in principle be attained with two complementary scenarios,<sup>2–6</sup> either by converting achiral substrates enantioselectively into chiral products (asymmetric induction) with the aid of an external chiral catalyst, or by taking advantage of enantiomers of racemic substrates or their derived products reacting with different rates under a chiral environment generated by an external catalyst (kinetic resolution). Strikingly, literature data accumulated from extensive studies on both AE and AD in the past decades revealed a nearly orthogonal stereochemical picture: while in asymmetric induction, AE only works well on allylic alcohols it has been demonstrated to be highly successful in kinetic resolutions of several classes of substrate structures; by contrast, as visualized in Fig. 1, while in asymmetric induction, with the aid of so-called commercial ‘AD-mix- $\alpha$  or  $\beta$ ’ reagent (bis-cinchona alkaloid–OsO<sub>4</sub> complex), AD consistently yields high ees over an enormously broad spectrum of

alkene substrates, kinetic resolution by means of this fundamental asymmetric catalysis technology has thus far only recorded very limited success.<sup>2</sup> The reasons for this have not yet been understood. To date, only a few reports on scattered substrate structures were known,<sup>2,7–23</sup> and the uncovered kinetic resolution efficiencies were relatively low. Consequently, there has been a growing belief that realizing general and highly effective AD-based kinetic resolution processes—if not impossible—can be rather difficult.<sup>2</sup>

*Introduction to the electronic helix theory:* a few years ago one of us (DZW) had published a new electronic helix theory for

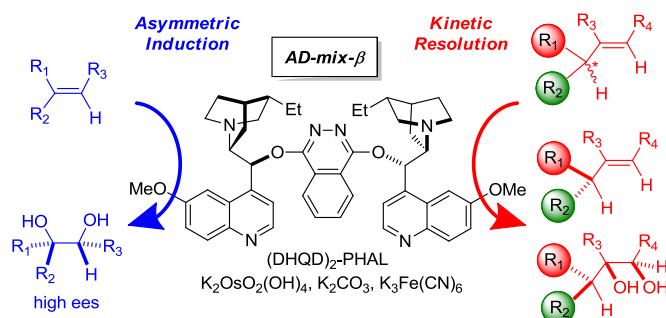


**Fig. 1.** Stereochemical duality in the Sharpless asymmetric dihydroxylation reactions: asymmetric induction versus kinetic resolution. (DHQD)<sub>2</sub>-PHAL stands for the phthalazine (PHAL) adduct with dihydroquinidine (DHQD).

\* Corresponding author. Tel.: +86 755 26035307; fax: +86 755 26032702; e-mail addresses: dzw@pkusz.edu.cn, dzw@szpku.edu.cn (D.Z. Wang).

molecular chirality and chiral interactions.<sup>23–28</sup> That theory illustrated the following three major points: one, chirality is helicity, and vice versa. Electronically they are just the same thing, thus structurally diverse molecular chiralities can be generalized on the basis of their inherent electronic helicities, being simply either right- or left-handed (Fig. 2A).<sup>23,25</sup> Such helicity could in turn be analyzed and identified from molecular electronic polarizability properties; two, within a pair of diastereomeric molecular interactions, such as those encountered in competing diastereomeric transition states in an asymmetric reaction, the interaction between molecules having the same helical handedness (i.e., homohelical interaction) is electronically always lower in energy than that with opposite handedness (hetero-helical interaction). That is, the principle underlying a chiral induction or recognition event is suggested to be the conservation of molecular electronic helicity.<sup>23,25</sup> An illustration of this helicity conservation principle is presented in Fig. 2B, in which the homohelical electronic inductions in asymmetric hydrogenation of simple ketones executed by a right-handed diphosphine diamine Ru catalyst all lead to chiral alcohol products of the same indicated absolute stereochemistry. What is notable in this exemplifying system is the demonstration of substrate electronic polarizability—but not its size—as a critical factor deciding the sense and magnitude of enantioselection. For **B1** and

**B2**, conventional steric rationale would predict wrong stereochemistry; and for **B3** and **B4**, it is unclear how enantioselection could originate from substrates featuring nearly isosteric substituents. By contrast, a polarizability-based stereochemical model<sup>23</sup> has proven to be generally applicable and predictive as in each of these cases the ketone substituent on the left (blue) is more polarizable than that on the right (red), and for the first time it helps explain why the foundation of current success in asymmetric catalysis in general appears to be closely associated with substrates characterized by significant  $\pi$ -versus- $\sigma$  polarizability distinctions (summarized as structure **B5**). Three, the homohelical-versus-heterohelical energetic difference, thus accordingly the magnitude of enantioselection in an asymmetric reaction, could be maximized when the interacting helices are energetically equal to each other (which is the case of, for example, autocatalysis).<sup>24,26</sup> As a chiral molecule's electronic helicity is closely derived from its polarizability characteristics, this helix theory is in essence an extension of Pearson's classical hard and soft acid and base (HSAB) theory into the three dimensional chiral space.<sup>26</sup> It is notable that molecular chirality is conventionally thought to be a solely geometrical property, and accordingly, chiral molecular interactions are usually analyzed by considering steric effects, thus our work has added useful electronic elements back to chiral systems. Indeed, applying this theory to an extensive range of major experiments<sup>23</sup> reported since the birth of asymmetric catalysis in 1960s showed that it is powerfully predictive and also accommodates results that conventional steric reasoning cannot.<sup>27,28</sup>

## 2. Results and discussion

*Design concept for Sharpless AD-based kinetic resolutions:* intrigued by the fascinating asymmetric induction-versus-kinetic resolution stereochemical phenomenon highlighted in Fig. 1, we initiated a program aimed at exploring the possibility of realizing highly efficient kinetic resolution systems based on the AD reactions. In this context, our efforts were critically guided by insights gained from electronic helix analysis on the AD systems,<sup>23,28</sup> which, as a conceptual reminiscence of an earlier stereochemical model<sup>29</sup> originated by Lohray et al., points to the importance of the engagement of electron-deficient hetero-aromatic linker unit (i.e.,  $\pi$ -character phthalazine moiety, Fig. 1) in the bis-cinchona alkaloid ligand towards  $\pi$ - $\pi$  stacking with an alkene substrate's electron-rich double bond. Within this context, we have recently been able to advance successfully a new polarizability-based stereochemical model for the Sharpless AD reactions.<sup>28</sup> As visualized in Fig. 3A, the AD-mix- $\beta$  reagent (DHQD)<sub>2</sub>-PHAL-OsO<sub>4</sub> featuring a right-handed electronic helicity<sup>23</sup> could be electronically represented by a simple  $\pi$ -chirality\*-N-OsO<sub>4</sub> diagram (in blue), thus in the illustrated catalyst-substrate interaction mode (Fig. 3B) the alkene double bond connects simultaneously with the catalyst through both complexation to OsO<sub>4</sub> and  $\pi$ - $\pi$  stacking with its phthalazine (PHAL) ring. While such a dual control mechanism on the substrate double bond significantly facilitates enantio-facial control, as evidenced by the remarkable success achieved across a broad range of alkenes in classical AD reactions, it however electronically disregards a racemic substrate's chirality, that is, positioned outside of the catalyst-substrate interaction means, thus inevitably jeopardizing chiral recognition efficiency requisite for high levels of catalytic kinetic resolutions. A logical solution to this problem therefore invites consideration on a new design scenario that takes advantage of an appropriately chosen  $\pi$ -character R<sub>2</sub> allylic substituent: it is anticipated that an effectively operating  $\pi$ - $\pi$  stacking between R<sub>2</sub> and the catalyst PHAL ring should incorporate a substrate's chirality within the corresponding catalyst-substrate interaction framework, thereby soliciting highly efficient chiral recognition and subsequent kinetic resolutions (Fig. 3C). Indeed, a careful survey of

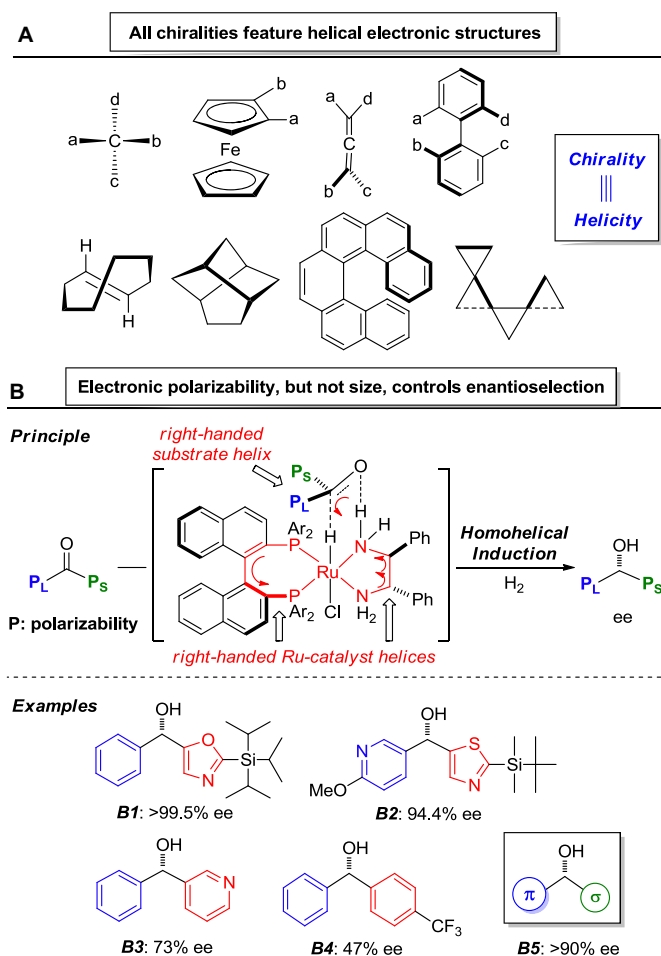


**Fig. 2.** Background information on a new electronic helix theory for molecular chirality and chiral interactions. A, Generalization of diverse molecular chiralities on the basis of their inherent electronic helicities. B, An illustration of homohelical electronic induction in diphosphine diamine Ru complex-catalyzed asymmetric hydrogenation of ketones: substituent polarizability plays more important role than its size in enantioselection.  $\pi$  denotes a  $\pi$ -electron cloud-containing substituent (such as aromatics, hetero-aromatics, ferrocenes, alkenes, or alkynes), and  $\sigma$  represents an alkyl group.  $P_L$ : substituent of larger polarizability;  $P_S$ : substituent of smaller polarizability.

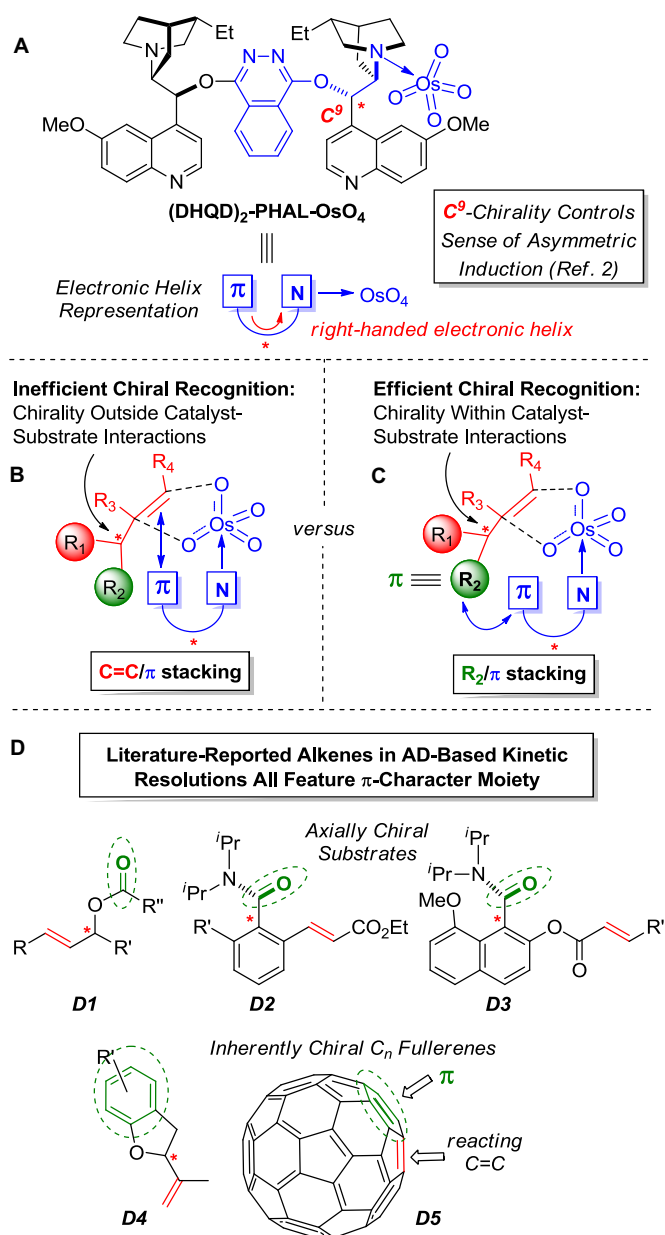


**Fig. 3.** A, The electronic helix representation of Sharpless AD-mix- $\beta$  reagent, which features a right-handed helicity,<sup>23</sup>  $\pi$  represent the hetero-aromatic phthalazine (PHAL) ring. B, Inefficient catalyst–substrate chiral recognition in kinetic resolution by means of the Sharpless asymmetric dihydroxylation reactions. C, A potential strategy for incorporating substrate chirality within catalyst–substrate interaction means through exploring  $\pi$ – $\pi$  stacking between catalyst PHAL ring and R<sub>2</sub> allylic substituent. D, Literature-reported substrates for AD-based kinetic resolutions that uniformly feature a  $\pi$ -character substituent (circled in green) adjacent to its reacting double bond. Star represents a chiral element; R<sub>1</sub>–R<sub>4</sub>, R, R', or R'' each denotes a substituent; for chiral C<sub>n</sub> fullerenes, n=76, 78, 84.

those reported alkenes in AD-based kinetic resolutions uniformly reveals the presence of a  $\pi$ -character group adjacent to its reacting double bond.<sup>2,7–23</sup> As circled in green in Fig. 3D, such a  $\pi$ -character moiety could be an ester carbonyl (D1), an amide carbonyl (D2 and D3), a benzene ring (D4), or a double bond (D5). Furthermore, in complete agreement with predictions from electronic helix analysis,<sup>23</sup> in each of these systems the recovered substrate enantiomer was the one that forms a homohelical recognition resting state with the right-handed AD-mix- $\beta$  reagent.

Guided by the above analysis, we set out to explore some racemic alkenes containing a  $\pi$ -character allylic substituent capable

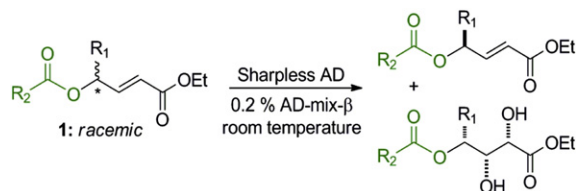
of participating on catalyst–substrate  $\pi$ – $\pi$  stacking in AD reactions. Our specific attention was placed on aryl rings flanked by both electron-donating and withdrawing substituents since their  $\pi$ -electronic clouds are considerably polarizable thus conducive for soliciting  $\pi$ – $\pi$  stacking interactions.<sup>30</sup> We reported herein that execution of this design scenario has proven to be fruitful: not only had we discovered that AD-based kinetic resolutions of such high-value structural motifs as allylic unsaturated esters were generally feasible, but also enantiomeric differentiation efficiencies in these processes were found to reach the highest levels known to date for chemical or even enzymatic kinetic resolution processes of any reaction type.<sup>31</sup>

**Kinetic resolutions of allylic unsaturated esters:** our investigations have chosen to focus on allylic unsaturated esters structured as **1** and the corresponding results were compiled in Table 1 (see Supplementary data for experimental details). Compound **1** contains several synthetically attractive and readily editable functionalities in its structure, including olefinic double bond,  $\alpha,\beta$ -unsaturated ester, allylic alcohol and its derived ester form. These recurring structural motifs are well represented in a diverse range of biologically and pharmaceutically meaningful natural products as well as their unnatural analogues or mimics. Recently disclosed examples are 16-membered trilactone macrolides macrophelides *A* and *E*,<sup>32</sup> antibacterial and antifungal agent botryolide *E*,<sup>33</sup> P-glycoprotein inhibitor taxane derivative related to taxuspine X,<sup>34</sup> anticancer agent brefeldin A and its ester derivatives,<sup>35</sup> and antibacterial cleistenolide against notably *Staphylococcus aureus* and *Bacillus anthracis*.<sup>36</sup> In contrast to **1**'s structural and functional significance, presently there are no effective catalytic asymmetric reaction methods known that could allow convenient access into these important chiral building blocks.

The kinetic resolution efficiency is characterized by the parameter termed selectivity factor *s*, which numerically is the ratio of (the rate of fast-reacting enantiomer)/(rate of slow-reacting enantiomer), and its quantity is calculated on the basis of the known equation  $s = \ln[(1-c)(1-ee)] / \ln[(1-c)(1+ee)]$ , where *ee* is the enantiomeric excess of the recovered substrate and *c* denotes the corresponding reaction conversion.<sup>37</sup> As with standard AD reactions employing as little as 0.2% mol of pseudo-enantiomeric AD-mix- $\alpha$  or  $\beta$  reagent for delivering high levels of asymmetric induction,<sup>2</sup> the experiments examined here also used this same low catalyst loading and run at room temperature for the sake of achieving reaction efficiency as well as operational practicality. Furthermore, particular attention was given to determining the selectivity factors associated with reaction conversions closely around 50% as enantio-purities of the recovered substrate tend to increase at the expense of higher reaction conversions, thus such *s* values measured at ~50% conversions are the more diagnostic indicators for the corresponding catalyst–substrate enantio-differentiation capacity thus the practical usefulness of the kinetic resolution process.<sup>37</sup> Additionally, it merits a note here that, although selectivity factor is a generally useful parameter for evaluating kinetic resolution process, its accurate determination depends on a detailed understanding of the rate laws of the reaction under concern and in some cases may become less straightforward.<sup>37</sup> Therefore, in the experiments shown below a list of *ee* deviations from the corresponding theoretical limit value at the given reaction conversion were tabulated alongside with the selectivity data to further aid the evaluation of kinetic resolution efficiency. Under such considerations we have established that an array of allylic unsaturated esters bearing different R<sub>2</sub>CO<sub>2</sub> and R<sub>1</sub> substitutions at the allylic carbons could be kinetically resolved with extremely high selectivity factors and enantioselectivities.

As summarized in Table 1, racemate **1** substituted with a piperonylate and a cyclopropyl ring (entry 1) underwent catalytic kinetic resolution with an extremely high selectivity factor of 213 under

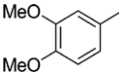
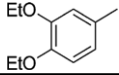
**Table 1**  
Kinetic resolution of allylic unsaturated esters by means of Sharpless asymmetric dihydroxylation (AD) reactions



Entry	R <sub>2</sub>	R <sub>1</sub>	s	ee of recovered substrate	Deviation to theor limit <sup>a</sup>
1			<b>194</b>	73.7% ee (43.0% conv)	1.7% ee
			<b>213</b>	98.1% ee (50.6% conv)	1.9% ee
			<b>194</b>	99.9% ee (52.3% conv)	0.1% ee
2			<b>166</b>	88.7% ee (47.9% conv)	3.2% ee
3			<b>45</b>	89.3% ee (50.5% conv)	10.7% ee
4			<b>21</b>	77.9% ee (49.5% conv)	20.1% ee
			<b>25</b>	89.4% ee (53.3% conv)	10.6% ee
5		CH <sub>3</sub> CH <sub>2</sub> -	<b>39</b>	83.6% ee (48.9% conv)	12.1% ee
			<b>24</b>	97.4% ee (58.1% conv)	2.6% ee
6			<b>301</b>	73.1% ee (42.6% conv) <sup>b</sup>	1.1% ee
			<b>213</b>	85.2% ee (46.6% conv) <sup>b</sup>	2.0% ee
			<b>198</b>	94.2% ee (49.4% conv) <sup>b</sup>	3.4% ee
			<b>261</b>	97.1% ee (50.1% conv) <sup>b</sup>	2.9% ee
			<b>170</b>	94.0% ee (49.5% conv)	4.0% ee
			<b>&gt;205</b>	>99.9% ee (51.8% conv)	0.0% ee
7			<b>138</b>	87.3% ee (47.6% conv)	3.5% ee
8			<b>75</b>	86.7% ee (48.3% conv)	6.7% ee
			<b>101</b>	95.5% ee (50.7% conv)	4.5% ee
9			<b>55</b>	80.4% ee (46.8% conv)	7.6% ee
			<b>68</b>	91.9% ee (50.3% conv)	8.1% ee
10		CH <sub>3</sub> CH <sub>2</sub> -	<b>32</b>	78.3% ee (47.6% conv)	12.5% ee
			<b>28</b>	97.1% ee (56.5% conv)	2.9% ee
11			<b>41</b>	90.1% ee (51.1% conv)	9.9% ee
			<b>47</b>	94.3% ee (52.3% conv)	5.7% ee
12			<b>156</b>	79.0% ee (44.9% conv)	2.5% ee
			<b>114</b>	95.4% ee (50.5% conv)	4.6% ee
13			<b>407</b>	96.8% ee (49.7% conv)	2.0% ee
			<b>139</b>	99.1% ee (51.7% conv)	0.9% ee
14			<b>53</b>	83.1% ee (47.8% conv)	8.5% ee
			<b>76</b>	89.6% ee (49.3% conv)	7.6% ee
15			<b>78</b>	84.3% ee (47.4% conv)	5.8% ee
			<b>79</b>	89.5% ee (49.1% conv)	7.0% ee
			<b>87</b>	93.9% ee (50.5% conv)	6.1% ee

(continued on next page)

Table 1 (continued)

Entry	R <sub>2</sub>	R <sub>1</sub>	s	ee of recovered substrate	Deviation to theor limit <sup>a</sup>
16		CH <sub>3</sub> CH <sub>2</sub> –	22	68.8% ee (45.4% conv)	14.3% ee
			28	90.9% ee (53.2% conv)	9.1% ee
			21	97.0% ee (59.1% conv)	3.0% ee
17			31	62.8% ee (41.6% conv)	8.4% ee
			70	85.5% ee (48.1% conv)	7.2% ee

<sup>a</sup> The ee deviation to the theoretical limit value at the same conversion is calculated by [ee(experiment)–ee(theory)].

<sup>b</sup> The catalyst here is AD-mix- $\alpha$ .

the action of 0.2 mol % of AD-mix- $\beta$  reagent, yielding the recovered substrate in 98.1% ee at 50.6% conversion. The selectivity factor was 194 with 73.7% ee being achieved at a conversion as low as 43.0%, which corresponded to a merely 1.7% ee deviation from the theoretical limit value of 75.4% ee at this same conversion. The enantioselection could be further improved to essentially 100% at 52.3% conversion while maintaining the selectivity factor at 194. Replacing the cyclopropyl ring with an isopropyl group resulted in a decreased selectivity factor at 166 (entry 2), but 88.7% ee was still achieved at 47.9% conversion, which was again only 3.2% ee away from the theoretical limit of 91.9% ee at this conversion. When R<sub>1</sub> varied among isobutyl, *n*-propyl and ethyl groups, the selectivity factors were in the range of 21–45 (entries 3–5). In marked contrast, when R<sub>1</sub> is cyclopropyl, replacing the piperonylate moiety with a 3,4-dimethoxybenzoate led to a significant increase of selectivity factor to 301 (entry 6), which ranks among the very few highest reported to date for kinetic resolution processes of any type, chemical or enzymatic.<sup>37</sup> This extreme catalyst–substrate chiral discrimination efficiency readily ensured 97.1% ee to be achieved at the practically significant 50.1% conversion. At 51.8% conversion, a nearly perfect >99.9% ee was recorded, and the corresponding selectivity factor became so large (>205) that it could not be calculated. Retaining the 3,4-dimethoxybenzene ring in **1** while changing the cyclopropyl to furan produced 87.3% ee at 47.6% conversion, thus constituting a selectivity factor of 138 (entry 7). From these results the important role of the R<sub>2</sub> aryl ring in modulating kinetic resolution efficacy clearly emerged, hence in entries 8–14 the R<sub>2</sub>CO<sub>2</sub>-moiety was replaced by six other aryl esters, including 6-methoxy-2-naphthoate, 6,7-dimethoxy-2-naphthoate, 4-methoxybenzoate, 3-bromo-4-methoxybenzoate, 3-iodo-4-methoxybenzoate and 2-methoxybenzoate. In each of these cases excellent selectivity factors ranging from 28 to 407 were recorded, demonstrating again the unique power of Sharpless AD reactions in effecting such kinetic resolutions. It should be noted here that the operation of electronic effects is transparent in these systems as earlier experiments with R<sub>2</sub> substituted with electron-withdrawing groups or with aliphatic R<sub>2</sub> all resulted in selectivity factors lower than 10. A further evidence was appreciable from results in entries 11–13, where the introduction of an electronically increasingly soft (i.e., more polarizable) bromo- and iodo-substituent, respectively, onto 4-methoxybenzoate dramatically enhanced the selectivity factors from 41 to 110 and then to 379 at about 50% conversions. Next, with 3,4-dimethoxybenzoate with an optimal allylic substitution, racemates **1** with branched (entry 15) or linear (entry 16) alkyl R<sub>1</sub> group were examined, and the corresponding selectivity factors, changing from 78–87 to 21–28, were found to respond somewhat sensitively to the steric effect perturbations, but these values remained to be practically significant and useful and high ees were consistently obtained around 50% conversions. A more pronounced steric effect was observed when a bulkier 3,4-diethoxybenzoate was employed, a comparison on entry 6 to entry 17 showed a marked decrease of selectivity factor from 170 to 70

within a comparable conversion range of 48–49%, but 85.5% ee of the recovered substrate was still realized at 48.1% conversion. Evidently, with such high levels of selectivity factors demonstrated in Table 1, the examined allylic unsaturated esters could all be obtained in enantio-pure form in the practically meaningful conversion range of 45–55%.

For kinetic resolutions reported in literature, it is rare that both the recovered substrate and the corresponding kinetically derived product could be obtained in high ees during the same reaction course.<sup>37</sup> In fact, none of the previously known AD-based kinetic resolutions had achieved ees over 90% with diol products of any type.<sup>2,7–23</sup> Thus, to examine this issue in the present systems, the stereoselections in the diol products **2** dihydroxylated from substrate **1** of entry 1 of Table 1 were carefully analyzed at different reaction conversions (Fig. 4A). Interestingly, at 35.5% conversion, the enantio-purities of the two diastereomers in the ratio of 8.6:1 were found to reach 99.9% ee (minor isomer) and 91.4% ee (major isomer), respectively. At 43.0% conversion, such high levels of ees were essentially preserved. At an even larger conversion of 50.6%, as might be well expected from the general kinetic resolution rate laws, the ees of the product diastereomers decreased slightly (to 90.0% and 80.0%, respectively) as the reaction progressed further. To the best of our knowledge, these findings represented the first examples demonstrating that, when such processes were intercepted at appropriate conversions, both recovered substrates and their diol products could be purposefully furnished in excellent enantio-purities.

Finally, the absolute stereochemical courses in these AD-based kinetic resolutions were probed by X-ray crystallographic analysis. To this end, we were able to grow single crystals of compounds **3** (R<sub>1</sub>=isopropyl) and **4** (R<sub>1</sub>=cyclopropyl) both prepared by derivatizing the diol products of **1** (entries 15 and 14, respectively, Table 1) with the chiral auxiliary (1*S*)-camphanic chloride, establishing unambiguously that the more reactive substrate enantiomer of **1** in both cases has the (*R*)-configuration at its allylic carbon and the produced major diol diastereomer has, in agreement with prediction from the Sharpless mnemonic device,<sup>2</sup> the expected (*S,S*)-configuration (Fig. 4B and C). It should be pointed out here that these stereochemical outcomes are again fully consistent with predictions from the electronic helix theory-based rationale, which was illustrated in Fig. 4D with **3** as a substrate. Because (*S*)-**3** possesses right-handed electronic helicity (polarizability rankings used for analyzing its helical handedness<sup>23</sup> are C=C>O, and <sup>i</sup>Pr>H) while interacting with the right-handed catalyst, thus it characterizes a homohelical recognition resting state with the AD-mix- $\beta$  reagent and is recovered, and accordingly (*R*)-enantiomer is kinetically derived into a diol product.

### 3. Conclusion

In summary, with new stereochemical insight gained from electronic helix theory as a critical guiding force, we have

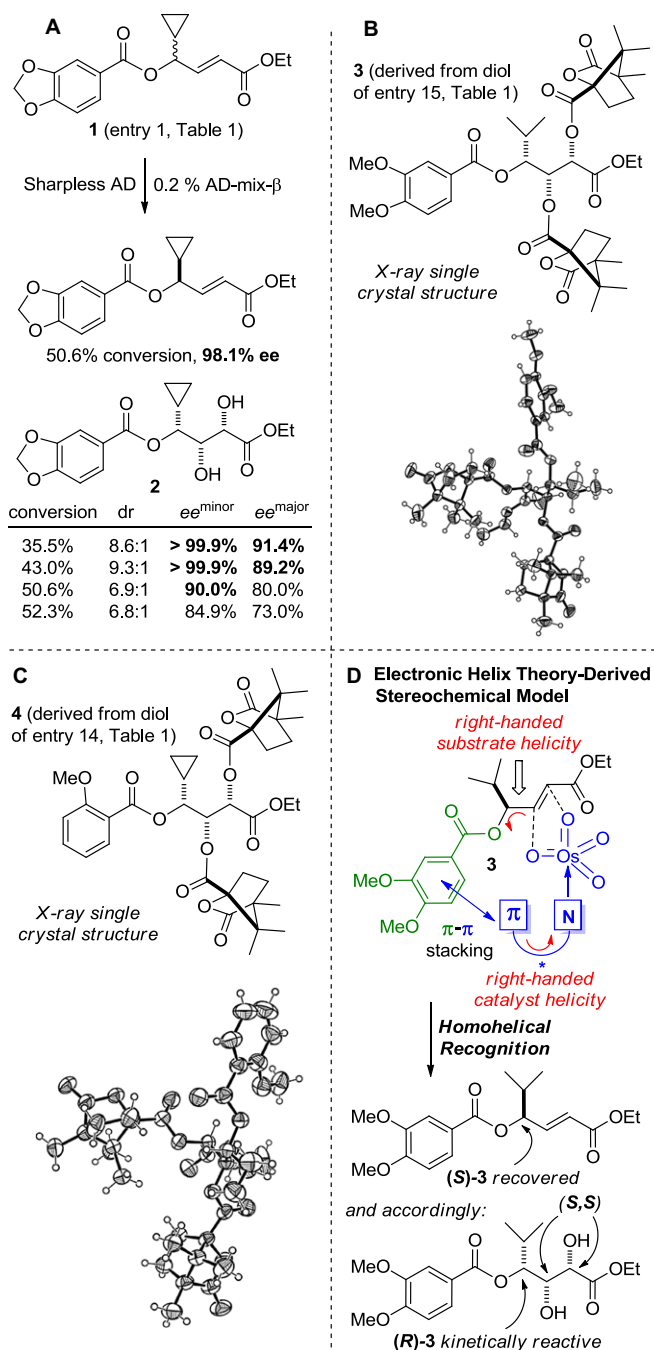


**Fig. 4.** A, Enantiomeric enrichment in a diol product **2** from the AD-based kinetic resolutions. B, Determination of the reaction absolute stereochemical course by X-ray crystallographic analysis of a diol-derived structure **3**. C, Determination of the reaction absolute stereochemical course by X-ray crystallographic analysis of a diol-derived structure **4**. D, An electronic helix theory-derived stereochemical model<sup>23</sup> for the observed highly efficient kinetic resolution in racemic **3**: right-handed (S)-substrate enantiomer forms a homohelical recognition resting state with the right-handed AD-mix- $\beta$  catalyst thus is recovered, and accordingly (R)-enantiomer is kinetically derived into a diol product.

demonstrated in these preliminary experiments that the long-pursued highly stereoselective catalytic kinetic resolution processes by means of the classical Sharpless asymmetric dihydroxylation reactions were not only generally feasible, but also with efficiencies up to the highest level known to date with chemical or even enzymatic kinetic resolutions of any reaction type. The discovery enables such versatile chiral building blocks as allylic unsaturated esters to be readily accessed with excellent enantiomeric

enrichments and at practically useful conversions, and further hints at the possible applicability of this new catalysis scenario to other types of important transformations, such as dynamic kinetic resolutions and kinetic desymmetrizations of olefin-containing compounds. Current efforts are thus directed at gaining a detailed understanding of the stereochemical control principle underlying these unusual kinetic reactivities and selectivities, as well as at expanding its substrate scope and practicality to prepare other high-value chiral substances.

## 4. Experimental

### 4.1. General experimental

Reagents were purchased at the highest commercial quality from Acros and Aldrich and used without further purification unless otherwise noted. Silica gel (ZCX-II, 200–300 mesh) used for flash column chromatography was purchased from Qing Dao Ocean Chemical Industry Co. <sup>1</sup>H and <sup>13</sup>C NMR spectra were recorded on a Bruker Avance III (300 MHz, 400 MHz or 500 MHz) spectrometers and are internally referenced to residual solvent signals (note: CDCl<sub>3</sub> referenced at  $\delta$  7.26 ppm for <sup>1</sup>H and  $\delta$  77.0 ppm for <sup>13</sup>C). Data for <sup>1</sup>H NMR are reported as follows: chemical shift ( $\delta$  parts per million), multiplicity (s=singlet, d=doublet, t=triplet, q=quartet, p=pentet, dd=doublet of doublets, ddd=doublet of doublet of doublets and m=multiplet), integration, coupling constant (hertz) and assignment. Data for <sup>13</sup>C NMR are reported in terms of chemical shift ( $\delta$  ppm). High resolution mass spectrometric (HRMS) data were obtained using Bruker Apex IV RTMS. High performance liquid chromatography (HPLC) was performed on a Shimadzu LC-20A using Daicel Chiralcell<sup>®</sup> chiral columns (25 cm) and guard column (5 cm) as noted for each compound. The room temperature (294 $\pm$ 1 K) single-crystal X-ray experiments were performed on a Bruker P4 diffractometer equipped with graphite monochromatized Mo K $\alpha$  radiation. Reagents were purchased at the highest commercial quality and used without further purification, unless otherwise stated. For full experimental details, including procedures for all reactions and characterizations of all new compounds (chiral HPLC analysis, <sup>1</sup>H NMR, <sup>13</sup>C NMR, mass spectrometry), X-ray single crystal structure analyses, see the [Supplementary data](#).

### 4.2. General procedure for kinetic resolutions of racemic **1** by means of the Sharpless asymmetric dihydroxylation (AD) reactions

Under a nitrogen atmosphere the olefin substrate (1 mmol) was dissolved in 7.1 mL of *t*-BuOH and 7.1 mL of H<sub>2</sub>O (0.07 M),<sup>2</sup> 1.4 g AD-mix- $\beta$  (or AD-mix- $\alpha$  as indicated, 0.2 mol %) and 1 mmol methanesulfonamide was added, respectively, the reaction mixture was stirred at room temperature. Aliquots were removed at different times and immediately quenched by adding saturated Na<sub>2</sub>SO<sub>3</sub>. The resultant mixture was extracted three times with ethyl acetate. The combined organic phase was washed with brine and then dried over anhydrous Na<sub>2</sub>SO<sub>4</sub> and concentrated to give a mixture containing both the residual olefin and the corresponding diol product. This mixture was analyzed directly by <sup>1</sup>H NMR spectroscopy to determine the conversion percentage. Then it was purified by column chromatography affording the recovered olefin and the diol product, whose enantio-purities were subsequently ascertained by chiral HPLC analysis (detailed HPLC conditions and results were compiled in the online [Supplementary data](#)). For each case reported in [Table 1](#) multiple sampling and NMR/HPLC analysis were performed to ensure data consistency and reproducibility, and the

selectivity factor values were the averages of at least 2 independent runs.

### Acknowledgements

Financial support was generously provided by the National Science Foundation of China (grants 20872004 and 20972008 to D.Z.W.), the National '973 Project' from the State Ministry of Science and Technology of China, the Shenzhen Bureau of Science, Technology and Information, and the Shenzhen 'Shuang Bai Project'. We also thank Professor R.-J. Wang (Tsinghua University Chemistry Department, X-Ray Diffraction Facility) and Professor T. Wang (Peking University Shenzhen Graduate School, Structural Biology Unit) for performing crystallographic analysis on **3** and **4**, respectively.

### Supplementary data

Detailed experimental procedures, single crystal X-ray structural analysis data, new compound characterization data, and copies of  $^1\text{H}$  and  $^{13}\text{C}$  NMR spectra. Supplementary data related to this article can be found online at <http://dx.doi.org/10.1016/j.tet.2012.06.102>.

### References and notes

1. Sharpless, K. B. *Angew. Chem., Int. Ed.* **2002**, *41*, 2024–2032.
2. Kolb, H. C.; VanNieuwenhze, M. S.; Sharpless, K. B. *Chem. Rev.* **1994**, *94*, 2483–2547.
3. Jacobsen, E. N., Pfaltz, A., Yamamoto, H., Eds.; Springer: Berlin, 1999; Vol I–III.
4. *Catalytic Asymmetric Synthesis*; Ojima, I., Ed.; Wiley-VCH: New York, NY, 2000.
5. Noyori, R. *Asymmetric Catalysis in Organic Synthesis*; Wiley: New York, NY, 1994.
6. For a leading reference on kinetic resolution, see: Kagan, H. B.; Fiaud, J. C. In: Allinger, N. L., Eliel, E. L., Eds. *Topics in Stereochemistry*; Wiley-Interscience: New York, NY, 1987; Vol. 14, p 249.
7. VanNieuwenhze, M. S.; Sharpless, K. B. *J. Am. Chem. Soc.* **1993**, *115*, 7864–7865.
8. Hawkins, J. M.; Meyer, A. *Science* **1993**, *260*, 1918–1920.
9. Lohray, B. B.; Bhushan, V. *Tetrahedron Lett.* **1993**, *34*, 3911–3914.
10. Crispino, G. A.; Makita, A.; Wang, Z.-M.; Sharpless, K. B. *Tetrahedron Lett.* **1994**, *35*, 543–546.
11. Corey, E. J.; Noe, M. C.; Guzman-Perez, A. *J. Am. Chem. Soc.* **1995**, *117*, 10817–10824.
12. Gardiner, J. M.; Norret, M.; Sadler, I. H. *Chem. Commun.* **1996**, 2709–2710.
13. Bakkeren, F. J. A. D.; Klunder, A. J. H.; Zwanenburg, B. *Tetrahedron* **1996**, *52*, 7901–7912.
14. Brimble, M. A.; Johnston, A. D. *Tetrahedron: Asymmetry* **1997**, *8*, 1661–1676.
15. Yokomatsu, T.; Yamagishi, T.; Sada, T.; Suemune, K.; Shibuya, S. *Tetrahedron* **1998**, *54*, 781–790.
16. Christie, H. S.; Hamon, D. P. G.; Tuck, K. L. *Chem. Commun.* **1999**, 1989–1990.
17. Yamaguchi, S.; Muro, S.; Kobayashi, M.; Miyazawa, M.; Hirai, Y. *J. Org. Chem.* **2003**, *68*, 6274–6278.
18. Hamon, D. P. G.; Tuck, K. L.; Christie, H. S. *Tetrahedron* **2001**, *57*, 9499–9508.
19. Rios, R.; Jimeno, C.; Carroll, P. J.; Walsh, P. J. *J. Am. Chem. Soc.* **2002**, *124*, 10272–10273.
20. Dai, W.-M.; Zhang, Y.; Zhang, Y. *Tetrahedron: Asymmetry* **2004**, *15*, 525–535.
21. Fleming, S. A.; Liu, R.; Redd, J. T. *Tetrahedron Lett.* **2005**, *46*, 8095–8098.
22. Bueno, A.; Rosol, M.; García, J.; Moyano, A. *Adv. Synth. Catal.* **2006**, *348*, 2590–2596.
23. Wang, D. Z. *Tetrahedron* **2005**, *61*, 7125–7133 and its online supporting material.
24. Wang, D. Z. *Tetrahedron* **2005**, *61*, 7134–7143.
25. Wang, D. Z. *Mendeleev Commun.* **2004**, *6*, 244–247.
26. Wang, D. Z. *Chirality* **2005**, *17*, 177–182.
27. Rouhi, A. M. *Chem. Eng. News* **September 29 2003**, 34–35.
28. Han, P.; Wang, R.-J.; Wang, D. Z. *Tetrahedron* **2011**, *67*, 8873–8878.
29. Lohray, B. B.; Bhushan, V. *Tetrahedron Lett.* **1992**, *33*, 5113–5116.
30. Prout, C. K.; Wright, J. D. *Angew. Chem., Int. Ed. Engl.* **1968**, *7*, 659–667.
31. Tokunaga, M.; Larrow, J. F.; Kakiuchi, F.; Jacobsen, E. N. *Science* **1997**, *277*, 936–938.
32. Prasad, K. R.; Gutala, P. *Tetrahedron* **2011**, *67*, 4514–4520.
33. Reddy, D. K.; Shekhar, V.; Prabhakar, P.; Babu, D. C.; Ramesh, D.; Siddhardha, B.; Murthy, U. S. N.; Wenkarteswarlu, Y. *Bioorg. Med. Chem. Lett.* **2011**, *21*, 997–1000.
34. Castaglione, D.; Contimori, L.; Maccari, G.; Avramova, S. I.; Neri, A.; Sgaragli, G.; Botta, M. *ACS Med. Chem. Lett.* **2010**, *1*, 416–421.
35. Anadu, N. O.; Davisson, V. J.; Cushman, M. *J. Med. Chem.* **2006**, *49*, 3897–3905.
36. Babu, D. C.; Selavam, J. J. P.; Reddy, D. K.; Shekhar, V.; Venkateswarlu, Y. *Tetrahedron* **2011**, *67*, 3815–3819.
37. Keith, J. M.; Larrow, J. F.; Jacobsen, E. N. *Adv. Synth. Catal.* **2001**, *343*, 5–26.